Supplementary Material

Main document: *A compositional model to assess expression changes from single-cell RNA-seq data*

Authors: Ma, Korthauer, Kendziorski, and Newton

Version: July 29, 2020.

This supplement is organized to match the sectioning of the main document. In summary,

1. Introduction
   - R package scDDboost
2. Modeling
   - 2.1 Data Structure, Sampling Model, and Parameters
     Illustrating key issue
     Proof of Theorem 2
   - 2.2 Method Structure and Clustering
     EBSeq
     modalClust
     Randomized distances
     Selecting K
     Robustness by randomized distances
   - 2.3 Double Dirichlet Mixture
     Proof of Properties 1-6 and Theorem 3
3. Numerical Experiments
   - 3.1 Synthetic data, splatter
   - 3.2 Empirical study, conquer and Null case
   - 3.3 Bursting
   - 3.4 Time complexity
   - 3.5 Diagnostics
     - Negative binomial assumption
     - Constant shape assumption
     - Clustering
4. Posterior consistency
   - Proof of Theorem 4

1. Introduction.

1.1. *R package.* R package `scDDboost` has tools for an end-to-end analysis of differential distribution via the proposed methodology. This includes clustering of unlabeled cells, `EBSeq` to assess probabilities of DE mean patterns among clusters, and final DD posterior probabilities. See https://github.com/wiscstatman/scDDboost

2. Modeling.

2.1. *Data Structure, Sampling Model, and Parameters.*

Illustrating key issue. Consider an example as in Figure 2 [main] wherein there are $K = 7$ subtypes having proportions $\phi = (\phi_1, \cdots, \phi_7)$ in one condition and different proportions $\psi = (\psi_1, \cdots, \psi_7)$ in the other. Though $\phi \neq \psi$, the marginal distribution of data at one gene may not differ between the conditions; this depends on ties that may exist in the seven component distributions. For demonstration's sake, suppose that there are three distinct component distributions among the seven, say $\alpha(x), \beta(x)$, and $\gamma(x)$, and suppose there are ties:

$$
\begin{aligned}
\alpha &= f_{g,3} = f_{g,4} \\
\beta &= f_{g,2} = f_{g,5} = f_{g,6} \\
\gamma &= f_{g,1} = f_{g,7}.
\end{aligned}
$$

These ties represent the lack of differential expression between subtypes within each block, but there are differences between blocks since α, β, and γ are all different. For the negative binomial model assumed in main, equalities and inequalities of component distributions correspond to equalities and inequalities of component means, as the shape is assumed constant within each gene. Let's work out the marginal distribution of data in the first condition, $f_g^1(x)$, noting the proportion constraints in Figure 2:

$$
\begin{aligned}
f_g^1(x) &= \sum_{k=1}^7 \phi_k f_{g,k}(x) \\
&= (\phi_3 + \phi_4)\alpha(x) + (\phi_2 + \phi_5 + \phi_6)\beta(x) + (\phi_1 + \phi_7)\gamma(x) \\
&= \Phi_{3,4}\alpha(x) + \Phi_{2,5,6}\beta(x) + \Phi_{1,7}\gamma(x) \\
&= \Psi_{3,4}\alpha(x) + \Psi_{2,5,6}\beta(x) + \Psi_{1,7}\gamma(x) \\
&= f_g^2(x).
\end{aligned}
$$

To reiterate the key issue, a gene that does not distinguish several subtypes (it has ties in the component distributions) does not distinguish the conditions even if there are different overall proportions, as long as certain aggregate proportions are unaltered.

PROOF OF THEOREM 2. Recall the parameters $\theta = (\phi, \psi, \mu, \sigma)$ and the dependence structure among variables indicated in the directed graph in Figure 3. We observe cell (sample) labels y_c, which accumulate into sample sizes n_1 and n_2 (numbers of cells within

each condition). Conditionally on these labels (and counts) subtype count vectors z^1, z^2 are multinomial draws given frequencies ϕ and ψ. Given subtype of a cell, measured expression $X_{g,c}$ follows a negative binomial distribution with mean depending on the gene and on the cell subtype. Thus $P(X, y, z|\theta) = P(y, z|\phi, \psi)P(X|z, \mu, \sigma)$. Further, (μ, σ) and (ϕ, ψ) are taken independent a priori given pattern π. By Bayes's rule (and always conditioning on π),

$$P(\theta|X, y, z) \propto P(X, y, z|\theta)P(\theta)$$
$$P(X, y, z|\theta)P(\theta) = P(y, z|\phi, \psi)P(X|z, \mu, \sigma)P(\mu, \sigma|z)P(\phi, \psi)$$
$$P(\phi, \psi|y, z) \propto P(y, z|\phi, \psi)P(\phi, \psi)$$
$$P(\mu, \sigma|X, z) \propto P(X|z, \mu, \sigma)P(\mu, \sigma|z)$$
$$\text{Thus } P(\theta|X, y, z) \propto P(\phi, \psi|y, z)P(\mu, \sigma|X, z)$$

It thus follows by integration over the parameter space that $P\left(A_\pi \cap M_{g,\pi}|X, y, z\right) = P\left(A_\pi|y, z\right) P\left(M_{g,\pi}|X, z\right)$. $\qquad\square$

2.2. *Method Structure and Clustering.*

EBSeq. Here we recall some key elements from Leng et al. (2013) on the model behind `EBSeq`, which we adapt to get $P(M_{g,\pi}|X, z)$. Suppose we have K subtypes, let $X_g^I = X_{g,1}^I, \cdots, X_{g,S_1}^I$ denote transcripts at gene g from subtype $I, I = 1, \cdots, K$. The `EBSeq` model assumes that normalized counts within subtype I are distributed as Negative Binomial: $X_{g,s}^I|\sigma_g, q_g^I \sim NB(\sigma_g, q_g^I)$ with density $P(X_{g,s}^I|\sigma_g, q_g^I) = \binom{X_{g,s}+\sigma_g-1}{X_{g,s}}(1 - q_g^I)^{X_{g,s}^I}(q_g^I)^{\sigma_g}$

Following Leng et al. (2013), we assume a prior distribution on $q_g^I : q_g^I|\alpha, \beta^g \sim Beta(\alpha, \beta^g)$. The hyperparameter α is shared by the whole genome and β^g is gene-specific. We force the size factor to be 1 for all cells and use the same procedure as `EBSeq` to estimate the shape parameter σ_g. Namely, we have

1. gene-level sample mean $m_g = \frac{1}{n}\sum_{s=1}^n X_{g,s}$, where $n = n_1 + n_2$ is the total number of cells

2. average of sample variances over subtypes $v_g = \frac{1}{K}\sum_{I=1}^K v_g^I$.

3. v_g^I is the unadjusted sample variance for subtype I, i.e. $v_g^I = \frac{1}{n^I}\sum_{s, z_s=I}(X_{g,s} - m_g^I)^2$ where m_g^I is the sample mean within subtype I and n^I is the number of cells within subtype I.

We estimate the pooled over-dispersion rate by $o_g = \frac{v_g}{m_g}$ and obtain $\sigma_g = m_g\frac{o_g}{1-o_g}$ from the first moment of NB. Our aim is to quantify the expression pattern among K groups:

$$M_{g,\pi} = \{\theta \in \Theta : \mu_{g,k} = \mu_{g,k'} \iff k, k' \in b, b \in \pi\}.$$

For example, if $K = 3$, there are 5 expression patterns, which may be written equivalently

in terms of parameters q:

$$P1 : q_g^1 = q_g^2 = q_g^3$$
$$P2 : q_g^1 = q_g^2 \neq q_g^3$$
$$P3 : q_g^1 \neq q_g^2 = q_g^3$$
$$P4 : q_g^1 = q_g^3 \neq q_g^2$$
$$P5 : q_g^1 \neq q_g^2 \neq q_g^3 \text{ and } q_g^1 \neq q_g^3$$

In a pattern where two groups I and J share the same q_g the counts from these groups are essentially pooled: i.e. $X_g^{I,J}|\sigma_g, q_g \sim NB(\sigma_g, q_g)$, $q_g|\alpha, \beta^g \sim \text{Beta}(\alpha, \beta^g)$. The prior predictive function is

$$
\begin{aligned}
f(X_g^{I,J}) &= \int_0^1 P(X_g^{I,J}|r_g, q_g) \, P(q_g|\alpha, \beta^g) \, dq_g \\
&= \left[\prod_{s=1}^S \binom{X_{g,s} + \sigma_g - 1}{X_{g,s}} \right] \frac{Beta(\alpha + \Sigma_{s=1}^S \sigma_g, \beta^g + \Sigma_{s=1}^S X_{g,s})}{Beta(\alpha, \beta^g)}.
\end{aligned}
$$

Consequently, the prior predictive function for $P1, \cdots, P5$ takes a convenient form if we further treat the distinct q's as independently drawn from the common Beta mixing distribution:

$$h_1^g(X_g) = f(X_g^{1,2,3})$$
$$h_2^g(X_g) = f(X_g^{1,2})f(X_g^3)$$
$$h_3^g(X_g) = f(X_g^1)f(X_g^{2,3})$$
$$h_4^g(X_g) = f(X_g^{1,3})f(X_g^2)$$
$$h_5^g(X_g) = f(X_g^1)f(X_g^2)f(X_g^3)$$

where $h_k^g(X_g) = P(X_g|M_{g,\pi_k}, z)$ for the associated pattern π_k. Then the marginal distribution of count vector X_g is $\sum_{k=1}^5 p_k h_k^g(X_g)$, where the mixing mass $p_k = P(M_{g,\pi}|z)$ is shared by all genes. Then, the posterior probability of an expression pattern k is obtained by:

$$\frac{p_k h_k^g(X_g)}{\sum\limits_{l=1}^5 p_l h_l^g(X_g)}.$$

In the optimization for determining the hyperparameters (α, β^g, p), we use EM for the mixing proportions and we use in each cycle a single gradient ascent step for α and β^g, in contrast to a full root-finding step used by EBSeq.

modalClust. We review and extend Dahl's modal clustering procedure (Dahl (2009)). This extension is part of the default cell clustering method of scDDboost. It operates on data from one gene at a time, and extends to Poisson-distributed observations the modal-clust procedure.

Product Partition Model (PPM): Let $X = (X_1, X_2, ..., X_n)$ be a vector of data (say at one gene). Given a partition $\pi = \{S_1, \cdots, S_q\}$, where S_i are disjoint subsets of $\{1, 2, \cdots, n\}$ and $\bigcup_{i=1}^{q} S_i = \{1, 2, \cdots, n\}$, a PPM for X entails

$$p(X|\pi) = \prod_{i=1}^{q} f(X_{S_i})$$

where X_{S_i} is the vector of observations corresponding to the items of component S_i. The component likelihood $f(X_S)$ is defined for any non-empty component S and can take many forms. The partition π, which clusters cells, is the parameter we are interested in. Other parameters that may have been involved in the model are integrated out. (Note the partition here has no relation to the partition of subtypes, as, e.g. in Figure 3.)

When the prior distribution for a partition π also takes a product form then so does the posterior. We aim to compute the MAP partition (maximizing the posterior $p(\pi|X) \propto p(X|\pi)p(\pi)$) to be used as an initial estimated clustering. Dahl (2009) demonstrated that by some choice of f and prior of π, we can reduce the time complexity of finding the MAP partition to $O(n^2)$. The crucial condition for f is the **non-overlapping** condition: if X_{S_1} and X_{S_2} are overlapped in the sense that $\min\{X_{S_2}\} < \max\{X_{S_1}\} < \max\{X_{S_2}\}$ or $\min\{X_{S_1}\} < \max\{X_{S_2}\} < \max\{X_{S_1}\}$, let $X_{S_1^*}$ and $X_{S_2^*}$ be the sets of swapping one pair of those overlapped terms and keep the other unchanged. Then $f(X_{S_1})f(X_{S_2}) \leq f(X_{S_1^*})f(X_{S_2^*})$. Here we confirm the non-overlapping condition for Poisson-Gamma observations.

Under the non-overlapping condition of density kernel f, the MAP partition π satisfies that for any two blocks $b_1, b_2 \in \pi$, either $\max_{i \in b_1}(X_i) \leq \min_{j \in b_2}(X_j)$ or $\min_{i \in b_1}(X_i) \geq \max_{j \in b_2}(X_j)$. Thus we reduce the solution space and reduce the time complexity. In the Poisson-Gamma model we have:

$$X_i|\pi, \lambda \sim Poisson(X_i|\lambda_1 \mathbf{I}\{i \in S_1\} + \cdots + \lambda_q \mathbf{I}\{i \in S_q\})$$
$$\pi \sim p(\pi)$$
$$\lambda_j \sim Gamma(\alpha_0, \beta_0)$$

where $p(\pi) \propto \prod_{i=1}^{q} \eta_0 \Gamma(|S_i|)$. Integrate out λ, $f(X_S)$ is obtained as:

$$f(X_S) = \frac{\beta^\alpha}{(|S| + \beta)^{\sum_{i \in S} X_i + \alpha}} \frac{\Gamma(\sum_{i \in S} X_i + \alpha)}{\Gamma(\alpha)} \frac{1}{\prod_{i \in S} X_i}$$

To apply modal-clustering on Poisson-Gamma model, we need to show the kernel $f(X_S)$ satisfies the non-overlapping condition.

Proof. If X_{S_1} and X_{S_2} are overlapping, without loss of generality, we assume $\min\{X_{S_2}\} < \max\{X_{S_1}\} < \max\{X_{S_2}\}$. To resolve the overlapping state, we could either swap the max element of S_1 with the min element of S_2 or the max element of S_2 while keeping the rest unchanged. Let S_1^* and S_2^* be the sets formed by swapping the max element of S_1 with the min element of S_2. Let S_1^{**}, S_2^{**} be the sets formed by swapping the max element of S_1 with the max element of S_2.

We need to show at least one of the following holds

(1) $$f(X_{S_1^*})f(X_{S_2^*}) \geq f(X_{S_1})f(X_{S_2})$$

(2) $$f(X_{S_1^{**}})f(X_{S_2^{**}}) \geq f(X_{S_1})f(X_{S_2})$$

Let $a = \max\{X_{S_1}\}$, $b = \min\{X_{S_2}\}$ and $c = \max\{X_{S_2}\}$, we have $b < a < c$. Let $h_1 = \sum_{i \in S_1} X_i - a$ and $h_2 = \sum_{i \in S_2} X_i - b$, n_1 and n_2 are the number of elements in S_1 and S_2. Then (1) can be equivalently expressed as

$$f(X_{S_1^*})f(X_{S_2^*}) \geq f(X_{S_1})f(X_{S_2})$$

$$\Longleftrightarrow$$

$$\frac{\Gamma(h_1 + a + \alpha)}{(n_1 + \beta)^{h_1 + a + \alpha}} \frac{\Gamma(h_2 + b + \alpha)}{(n_2 + \beta)^{h_2 + b + \alpha}} \leq \frac{\Gamma(h_2 + a + \alpha)}{(n_2 + \beta)^{h_2 + a + \alpha}} \frac{\Gamma(h_1 + b + \alpha)}{(n_2 + \beta)^{h_1 + b + \alpha}}$$

$$\Longleftrightarrow$$

$$\frac{\Gamma(h_1 + a + \alpha)}{\Gamma(h_1 + b + \alpha)} \frac{\Gamma(h_2 + b + \alpha)}{\Gamma(h_2 + a + \alpha)} \leq \left(\frac{n_1 + \beta}{n_2 + \beta}\right)^{a-b}$$

The left hand side of the above formula is $\text{LHS}_1 = \frac{(h_1+b+\alpha)...(h_1+a-1+\alpha)}{(h_2+b+\alpha)...(h_2+a-1+\alpha)}$ by the property of Gamma function and that X_i are integers.

Similarly, (2) can be equivalently expressed as

$$f(X_{S_1^{**}})f(X_{S_2^{**}}) \geq f(X_{S_1})f(X_{S_2})$$

$$\Longleftrightarrow$$

$$\frac{\Gamma(h_2 + c + \alpha)}{\Gamma(h_2 + a + \alpha)} \frac{\Gamma(h_1 + a + \alpha)}{\Gamma(h_1 + c + \alpha)} \leq \left(\frac{n_2 + \beta}{n_1 + \beta}\right)^{c-a}$$

The left hand side of above formula is $\text{LHS}_2 = \frac{(h_2+a+\alpha)...(h_2+c-1+\alpha)}{(h_1+a+\alpha)...(h_1+c-1+\alpha)}$.

If $h_1 \leq h_2$, then $\text{LHS}_1 \leq \left(\frac{h_1+a-1+\alpha}{h_2+a-1+\alpha}\right)^{a-b}$ and $\text{LHS}_2 \leq \left(\frac{h_2+c-1+\alpha}{h_1+c-1+\alpha}\right)^{c-a}$.

So if $\frac{h_1+a-1+\alpha}{h_2+a-1+\alpha} \leq \frac{n_1+\beta}{n_2+\beta}$ then (1) holds, if $\frac{h_2+c-1+\alpha}{h_1+c-1+\alpha} \leq \frac{n_2+\beta}{n_1+\beta}$ then (2) holds.

We multiply those two inequalities, and find that the left hand side $\frac{h_1+a-1+\alpha}{h_2+a-1+\alpha} \frac{h_2+c-1+\alpha}{h_1+c-1+\alpha} = \frac{h_1+a-1+\alpha}{h_1+c-1+\alpha} \frac{h_2+c-1+\alpha}{h_2+a-1+\alpha} \leq 1$ as $c > a$ and $h_1 \leq h_2$. But the right hand side $\frac{n_1+\beta}{n_2+\beta} \times \frac{n_2+\beta}{n_1+\beta} = 1$. Consequently at least one of (1) and (2) holds.

The proof for case $h_1 > h_2$ follows similarly.

$\square$

Randomized distances. `scDDboost` reports average posterior probabilities, where the averaging is taken over clusterings of cells induced from randomized distance matrices. A Bayesian argument for this technique is presented in the Appendix. Random distance $d_{i,j}^* = d_{i,j}/w_{i,j}$, where $w_{i,j} = e_i + e_j$ and the $\{e_i\}$ are random Gamma$(a/2, a)$ deviates. Parameter a is estimated by an empirical Bayes argument, using the deduction

$$(3) \qquad P(d_{i,j}|a_0, a_1, d_0) = \frac{\Gamma(a_0 + a_1)}{\Gamma(a_0)\Gamma(a_1)} \frac{d_0^{a_0} d_{i,j}^{a_1-1} a_1^{a_1}}{(d_0 + a_1 d_{i,j})^{a_0+a_1}}$$

for parameters a_0, a_1, and d_0, and recognizing $a = a_0 + a_1$. We estimate these parameters from the collection of observed distances $\{d_{i,j}\}$. First d_0 is estimated by the method of moments, noting $d_0 = E(1/d_{i,j})/var[1/d_{i,j}]$. Next we estimate a_0 and a_1 by optimization of a marginal log-likelihood using (3) and program `nlminb` in `R`. We limit tolerance to avoid overflow issues. Supplementary Figure S1 shows the level of variation in clusterings produced by this randomized distance approach in 8 example data sets.

We further check validity of randomized distances as a Bayesian approximation by comparing it to Dirichlet-process-based clustering (Jara et al. (2011)) on a simulated dataset. We simulate one-dimensional data X from a mixture of 5 normal distributions with different means and same variance ($\mu = (-6, -2, 0, 2, 10), \sigma = 1$). We compare clustering results between randomized distances and Bayesian clustering using the Dirichlet process prior (using `DPpackage`) in terms of posterior probabilities that two elements belong to the same class given the whole data. We also compare accuracy of the two procedures by looking at the ARI comparing to true class label (Supplementary Figure S2). We find that randomized distance scheme closely matches the distributional features of the Dirichlet-process computation, and, in this case, tends to put more mass close to the data-generating partition.

Selecting K. In this section, we give the criterion to select the number of subtypes K. We implement a procedure inspired by `validity`, as defined in Ray and Turi (2000). We consider a modified `validity`= $\frac{\text{intra}}{\text{inter}}$, where **intra** = $\frac{1}{N} \sum_{i=1}^{K} \sum_{x \in C_i} ||x - z_i||^2$, **inter** = mean$(||z_i - z_j||^2), i, j = 1, 2, ...K$, and z_i is the center (medoid) of cluster i. **intra** is the average of distance of a point to the center of its corresponding cluster, which measures the compactness of clusters. **inter** is the average distance between centers, which measures the separation between clusters. In the original paper **inter** was defined as minimum distance between medoids (Ray and Turi, 2000). Here, we instead use the average for smoothness. By minimizing `validity` (contrary to what the name suggests) we aim for small intra-cluster distance and large inter-cluster distance. We find empirically that `validity` is monotonic decreasing with K and this trend stabilizes when K is sufficiently big. We select the first K satisfying `validity`$_K < \epsilon$. We set the default value of ϵ to be 1, as we found this yields good performance in simulation.

Supplementary Figure S1: Adjusted RAND index of clusterings generated by randomizing distances. The plot shows variation of clustering induced by randomizing distance matrices in 8 data sets and for 100 randomized matrices per data set. In each data set, ARI is computed between the clusterings from all randomized distances and the clustering induced by the non-randomized distance matrix.

Robustness. In this section, we demonstrate change of the posterior probability of DD under different K, and also the robustness provided by randomized distances. We also give an example where very large K inflates FDR.

The number of subtypes K is an important parameter. Taking K too small may end up underfitting such that cells within same subtype can still be very different, the mean expression change among subtypes is incapable to capture the marginal distribution change. This would lead to reduced power. Too large K may end up overfitting such that two subtypes can be very similar. Given that we have a fixed number of cells, allowing more clusters will not only increase the burden of computation but decrease the certainty of our inference on DE pattern. Empirically we find that taking $K \leq 10$ is often sufficient (Supplementary Table S1). In any case, we note here that K affects the posterior probability of DD (PDD).

To demonstrate the change of PDD over different K, we present an example using dataset GSE75748. When we increase K, the variance of the differential term $\text{PDD}_{K+1} -$

Supplementary Figure S2: Comparison between randomized distance scheme and Dirichlet-process procedure. Top: heatmap of probabilities that two elements belong to the same class given the whole data. Bottom: scatterplot of these posterior probabilities (left), and adjusted RAND index comparing to the underlying true class label (right).

PDD_K keeps decreasing and PDD keeps increasing. Our selection criterion (K = 5) happens to choose K such that change between PDD_{K+1} and PDD_K is small while not inflating PDD. We generally obtain stable validity score and PDD simultaneously (Supplementary Figure S3). In addition, the randomized distance scheme helps by smoothing PDD (Supplementary Figure S4).

scDDboost may lose FDR control if K is not maintained at a sufficiently small value. Supplementary Figure S5 shows what happens as K increases in one case, other factors staying constant. In our simulation study, we note that the validity score method was

always conservative, and did not lead to overestimating K.

Supplementary Figure S3: PDD change under different number of subtypes K for dataset DEC-EC (GSE75748). We select $K = 4$, which also stabilize the PDD.

Supplementary Figure S4: PDD under $K = 5$ vs. $K = 6$ for dataset DEC-EC (GSE75748). PDD without randomization (left) vs. PDD with randomization (right). `scDDboost` gained robustness through averaging over randomized distances.

2.3. *Double Dirichlet Mixture.* In this section, we give proofs for the properties of DDM in Section 2.3 of the main paper. Using notation from the main paper, we have density functions:

$$p_\pi(\phi, \psi) = q_\pi(\Phi_\pi, \Psi_\pi) \prod_{b \in \pi} [p(\tilde{\phi}_b) p(\tilde{\psi}_b)]$$

with

$$q_\pi(\Phi_\pi, \Psi_\pi) = \frac{\Gamma(\sum_{b \in \pi} \beta_b)}{\prod_{b \in \pi} \Gamma(\beta_b)} \left[\prod_{b \in \pi} \Phi_b^{\beta_b - 1} \right] 1\left[\Phi_\pi = \Psi_\pi\right]$$

and

$$p(\tilde{\phi}_b) = \frac{\Gamma(\sum_{k \in b} \alpha_k)}{\prod_{k \in b} \Gamma(\alpha_k)} \prod_{k \in b} \tilde{\phi}_k^{\alpha_k - 1}, \qquad p(\tilde{\psi}_b) = \frac{\Gamma(\sum_{k \in b} \alpha_k)}{\prod_{k \in b} \Gamma(\alpha_k)} \prod_{k \in b} \tilde{\psi}_k^{\alpha_k - 1}.$$

Supplementary Figure S5: FDR control may be lost if K is too large. Calculations here use dataset EMTAB2805null (Table S2) and target 5% FDR, which is not controlled when $K > 6$ But by the validity score method we would choose K much smaller, as that score stabilizes $K \geq 3$.

These serve as key components for proving DDM properties.

PROOF OF PROPERTY 1. When ϕ and ψ only satisfy the coarsest constraint: $\sum_{i=1}^{K} \phi_i = \sum_{i=1}^{K} \psi_i = 1$, then ϕ and ψ are independently Dirichlet distributed. Finer constraints will lead to dependency between ϕ and ψ as there is a proper subset b of π such that $\sum_{i \in b} \phi = \sum_{i \in b} \psi$, which make $P(\phi|\psi) \neq P(\phi)$. □

PROOF OF PROPERTY 2. By the law of total expectation, $E_\pi(\phi_k) = E_\pi(E_\pi((\phi_k|\Phi_b)) = E_\pi(E_{\tilde{\phi}_b}(\tilde{\phi}_k)) = E_{\tilde{\phi}_b}(\tilde{\phi}_k)E_\Phi(\Phi_b)$ where b is the block containing subtype index k. Since $\tilde{\phi}_b \sim \text{Dirichlet}_{N(b)}[\alpha_b^1]$ and $\Phi_\pi \sim \text{Dirichlet}_{N(\pi)}[\beta_\pi]$, we have $E_{\tilde{\phi}_b}(\tilde{\phi}_k) = \frac{\alpha_k^1}{\sum_{k' \in b} \alpha_{k'}^1}$, $E_\Phi(\Phi_b) = \frac{\beta_b}{\sum_{b' \in \pi} \beta_{b'}}$ and $E_\pi(\phi_k) = \frac{\alpha_k^1}{\sum_{k' \in b} \alpha_{k'}^1} \frac{\beta_b}{\sum_{b' \in \pi} \beta_{b'}}$. The case for $E_\pi(\psi_k)$ is similar. □

PROOF OF PROPERTY 3. t^1/t_π^1 is independent of t^2/t_π^2 conditioning on t_π^1 and t_π^2 by the neutrality property of Dirichlet distribution □

PROOF OF PROPERTY 4. For $j = 1, 2$, let T_b^j be the vector of t_k^j such that $k \in b$. Recall $t_b^j = \sum_{k \in b} t_k^j$. Without loss of generality, we consider the case condition $j = 1$. At the support of p_π, for different blocks, $T_b^1|\tilde{\phi}_b$ are mutually independent. Then we have factorization:

$$p_\pi(t^1|t_\pi^1, y) = \prod_{b \in \pi} p(T_b^1|t_b^1, y)$$

and right hand side prior predictive function can be obtained by integrating out $\tilde{\phi}_b$. Namely

$$
\begin{aligned}
p(T_b^1|t_b^1, y) &= \int_{\tilde{\phi}_b} p(T_b^1|\tilde{\phi}_b)p(\tilde{\phi}_b)d\tilde{\phi}_b \\
&= \left\{ \left[\frac{\Gamma(t_b^j + 1)}{\prod_{k \in b} \Gamma(t_k^j + 1)} \right] \left[\frac{\Gamma(\sum_{k \in b} \alpha_k^j)}{\prod_{k \in b} \Gamma(\alpha_k^j)} \right] \left[\frac{\prod_{k \in b} \Gamma(\alpha_k^j + t_k^j)}{\Gamma(t_b^j + \sum_{k \in b} \alpha_k^j))} \right] \right\}
\end{aligned}
$$

given the prior Dirichlet$[\alpha_b^1]$ of $\tilde{\phi}_b$ and that $p(T_b^1|\tilde{\phi}_b)$ is a multinomial$(\tilde{\phi}_b)$ distribution. $\square$

PROOF OF PROPERTY 5. t_π^1 and t_π^2, given the condition label y, are independent and identically distributed with $t_\pi^1|\Phi \sim$ multinomial(Φ). Thus

$$
\begin{aligned}
p_\pi(t_\pi^1, t_\pi^2|y) &= \int_\Phi p(t_\pi^1|\Phi)p(t_\pi^2|\Phi)p(\Phi)d\Phi \\
&= \left[\frac{\Gamma(n_1 + 1)\Gamma(n_2 + 1)}{\prod_{b \in \pi} \Gamma(t_b^1 + 1)\Gamma(t_b^2 + 1)} \right] \left[\frac{\Gamma(\sum_{b \in \pi} \beta_b)}{\prod_{b \in \pi} \Gamma(\beta_b)} \right] \left[\frac{\prod_{b \in \pi} \Gamma(\beta_b + t_b^1 + t_b^2)}{\Gamma(n_1 + n_2 + \sum_{b \in \pi} \beta_b)} \right].
\end{aligned}
$$

As prior of Φ is Dirchlet$[\beta]$ and $n_j = \sum_{b \in \pi} t_b^j$ for $j = 1, 2$. $\square$

To prove Property 6, we need a fact about dimensionality of the intersection of two A_π's.

LEMMA 1. *If π_2 is not a refinement of π_1 then $A_{\pi_1} \cap A_{\pi_2}$ is a lower dimensional subset of A_{π_2}.*

PROOF OF LEMMA 1. To formalize the problem in linear algebra, we consider the vector space R^{2K}, and define a map from block to vector in R^K :$g(b) = v_b$, where ith component of v_b is 1 if $i \in b$ and 0 otherwise.

Let V_1, V_2 denote the orthogonal space of $\phi - \psi$ when $(\phi, \psi) \in \cap A_{\pi_2}, A_{\pi_2}, A_{\pi_1}$. Notice that $\dim(A_{\pi_1} \cap A_{\pi_2}) = \dim(\phi - \psi) + \dim(\psi) = K - \dim(V_1) + K - 1 = 2K - \dim(V_1) - 1$, $\dim(A_{\pi_2}) = 2K - \dim(V_2) - 1$, $\dim(V_2) = N(\pi_2)$. Assuming $\pi_1 = \{b_1^1, \cdots, b_s^1\}$, and $\pi_2 = \{b_1^2, \cdots, b_t^2\}$. The corresponding vectors are $v_1^1, \cdots, v_s^1$ and $v_1^2, \cdots, v_t^2$. We claim there must be a $b_i^1 \in \pi_1$ whose corresponding vector v_i^1 is linear independent with $v_1^2, \cdots, v_t^2$. If not, for every v_i^1 there exists $\alpha_1^i, \cdots, \alpha_t^i$ such that

$$
(4) \qquad v_i^1 = \sum_{j=1}^{t} \alpha_j^i v_j^2
$$

If $b_j^2 \cap b_i^1 \neq \emptyset$, then $v_i^1 * v_j^2 > 0$ and we multiply v_j^2 on both sides of (4), we obtain $v_i^1 v_j^2 = \alpha_j^i(v_j^2)^2$, as $v_p^2 v_q^2 = 0$ if $p \neq q$. This implies $\alpha_j^i > 0$. Consider $x = g(b_j^2 \setminus b_i^1)$. We have $xv_i^1 = 0$ and multiply x on both sides of (4) to obtain $\alpha_j^i v_j^2 x = 0$. Thus x must be the zero vector and $b_j^2 \setminus b_i^1 = \emptyset$, which implies $b_j^2 \subset b_i^1$. That is to say when

$b_j^2 \cap b_i^1 \neq \varnothing$, b_j^2 must be a subset of b_i^1. So b_i^1 is the union of some blocks in π_2. This implies π_2 is a refinement of π_1, which is a contradiction. Consequently, there exists $b \in \pi_1$ whose v_b is linear independent with $v_{b'}, \forall b' \in \pi_2$. Thus the $\dim(V_1)$ is is at least $N(\pi_2) + 1, \dim(A_{\pi_1} \cap A_{\pi_2}) < \dim(A_{\pi_2})$. $\qquad\square$

PROOF OF PROPERTY 6. For any π, $P(A_\pi, |y, z) = \sum_{\tilde{\pi} \in \Pi} \int_{A_\pi} \omega_{\tilde{\pi}}^{\text{post}} d\phi d\psi$, notice the support of $\omega_{\tilde{\pi}}^{\text{post}}$ is $A_{\tilde{\pi}}$. By Lemma 1, we know if $\tilde{\pi}$ does not refine π, then $\int_{A_\pi} \omega_{\tilde{\pi}}^{\text{post}} d\phi d\psi$ is an integral on lower dimension set and vanishes. if $\tilde{\pi}$ refines π, then $\int_{A_\pi} \omega_{\tilde{\pi}}^{\text{post}} d\phi d\psi = \int_{A_{\tilde{\pi}}} \omega_{\tilde{\pi}}^{\text{post}} d\phi d\psi = \omega_{\tilde{\pi}}^{\text{post}}$. We have $P(A_\pi, |y, z) = \sum_{\tilde{\pi} \in \Pi} \omega_{\tilde{\pi}}^{\text{post}} 1[\tilde{\pi} \text{ refines } \pi]$. $\qquad\square$

PROOF OF THEOREM 3. Recall the DDM prior: $p(\phi, \psi) = \sum_{\pi \in \Pi} p_\pi(\phi, \psi)$. By Bayes's rule $p(\phi, \psi | y, z) \propto p(\phi, \psi, y, z) = \sum_{\pi \in \Pi} p(y, z | \phi, \psi) \, p_\pi(\phi, \psi) \omega_\pi$ and the 1-1 map from (ϕ, ψ) to $(\tilde{\phi}, \tilde{\psi}, \Phi)$, we have

$$p(y, z | \phi, \psi) p_\pi(\phi, \psi) = p(y, z | \tilde{\phi}, \tilde{\psi}, \Phi_\pi) \, p(\tilde{\phi}) \, p(\tilde{\psi}) \, p(\Phi_\pi)$$

when $(\phi, \psi) \in A_\pi$. Let us denote right hand side of the above equation as U_π, then

$$U_\pi = \omega_\pi A_1 A_2 A_3 \prod_{k=1}^{K} (\tilde{\phi}_k)^{t_k^1 + \alpha_k^1} (\tilde{\psi}_k)^{t_k^2 + \alpha_k^2} \prod_{b \in \pi} (\Phi_b)^{t_b^1 + t_b^2 + \beta_b},$$

where A_1 is the product of normalizing terms from multinomial distribution of z^1 and z^2, $A_1 = \frac{\Gamma(n_1 + 1)\Gamma(n_2 + 1)}{\prod_{j=1}^2 \prod_{k=1}^K \Gamma(t_k^j + 1)}$, and A_2 is the product of normalizing terms from Dirichlet distribution of $\tilde{\phi}$ and $\tilde{\psi}$, $A_2 = \frac{\Gamma(\sum_{k=1}^K \alpha_k^1 + 1)\Gamma(\sum_{k=1}^K \alpha_k^2 + 1)}{\prod_{j=1}^2 \prod_{k=1}^2 \Gamma(\alpha_k^j + 1)}$, and A_3 is the normalizing term from Dirichlet distribution of Φ_π, $A_3 = \frac{\Gamma(\sum_{b \in \pi} \beta_b + 1)}{\prod_{b \in \pi} \Gamma(\beta_b + 1)}$. Looking at the indices of $\tilde{\phi}, \tilde{\psi}$ and Φ, we can decompose U_π as a product of three Dirichlet densities with a normalizing term. Namely $U_\pi = C_\pi f_1 f_2 f_3$, where $f_1 \sim \text{Dirichlet}[\alpha^1 + t^1]$, $f_2 \sim \text{Dirichlet}[\alpha^2 + t^2]$ and $f_3 \sim \text{Dirichlet}[\beta + t^1 + t^2]$. Considering the normalizing factors for densities f_1, f_2 and f_3, and multiplying them with A_1, A_2 and A_3, we have $C_\pi = p_\pi(t^1 | t_\pi^1, y) \, p_\pi(t^2 | t_\pi^2, y) \, p_\pi(t_\pi^1, t_\pi^2 | y) \omega_\pi$. Consequently, we have

$$(\phi, \psi) | y, z \quad \sim \quad \text{DDM} \left[\omega^{\text{post}} = (\omega_\pi^{\text{post}}), \alpha^1 + t^1, \alpha^2 + t^2 \right] \qquad \text{and}$$

$$\omega_\pi^{\text{post}} \quad \propto \quad p_\pi(t^1 | t_\pi^1, y) \, p_\pi(t^2 | t_\pi^2, y) \, p_\pi(t_\pi^1, t_\pi^2 | y) \, \omega_\pi.$$

Notice in DDM, we restrict $\beta = \alpha^1 + \alpha^2$.

$\qquad\square$

3. Numerical Experiments.

3.1. *Synthetic Data.*   **Xiuyu; we base so much on how we operate on splatter-generated data, it is unfortunate that we do not have even a basic description of the model driving splatter. I invite you to write a few sentences here about that model; I think it is important for us to be able to say that the mixture model behind scDDboost is not the same as the model behind splatter...this is to our benefit when we see good operating characteristics; the paragraph you added so far is helfpul, but it still requires that we go back to the Zappia paper to know anything about the model underlying splatter. I think we need some sort of explanation in our paper. Thanks.**

In this section we look more closely at the synthetic data generated using `splatter`. `splatter` is a state of art simulation framework that approximates empirical data well. To make authentic data, gene expression of cells within the same group are generated through a multi-layer model, Those layers considering the state of whether it is an outlier or dropout, library size(sequencing depth) and trended gene-wise dispersion, which make the marginal expression distribution more complicate than the negative binomial model assumed by `scDDboost`. Input parameters for the multi-layer model are internally estimated using empirical data sets. However, for generating data of multiple groups, it requires user to provide a pair of location and scale parameters governing the intensity of DE for those signature genes that distinct each group. In summary, `splatter` take three parameters, the number of groups(clusters) and a pair of the location and scale parameters for multi-group simulation. To evaluate performance on the data sets with small number of clusters to relative large number of clusters, we consider the cases when the number of clusters is 3,7 and 12. For the choice of the hyperparamter pair, we use two settings suggested by `splatter`, which are (0.1,0.4) and (-0.1,0.3). However, those settings induce weak signal for DD and all methods have low power. For the sake of comparison between different DD methods, we amplify the evidence of DD by introducing two more hyperparameter pairs (0.3,0.5) and (-0.1,1).

PCA plots provide a global (transcriptomic) view of changes between splatter-simulated subtypes: Supplementary Figures S6, S7, S8 summarize the cases $K = 3, 7$, and 12, respectively. Parameter choices provide for some strong and some very weak differences. **Xiuyu: I don't see what distinguishes the top row of 4 PCA plots from the bottom row in each figure. Here, I guess, we could have some clarity; perhaps it refers to a pair of hyperparameters, but I cannot tell. Please advise. Thanks **

Supplementary Figure S9 confirms that the probability scores from `scDDboost` are associated with simpler measures on the magnitude of distributional change. These plots compare equivalence probabilities to empirical Wasserstein distance **Xiuyu: please provide a citation to this metric**

The main paper shows performance of `scDDboost` on simulated data in terms of false positive rates and power at specific thresholds. Alternatively, we may view it as more of a prediction problem and report receiver-operating-characteristic (ROC), as in Supplementary Figure S10. Each sub-figure corresponds to one of the parameter settings and reports an average over ten replicates under the same parameters setting. `scDDboost` tends to outperform other methods.

Supplementary Figure S6: First two principal components of transcripts under different parameters for simulated data. Horizontal axis refers to first component, vertical axis refers to second component. Different parameters resulted in different degree of separation of subtypes. We have 4 different settings for hyper-parameters of simulation, each setting has 10 replicates. From left to right, the associated hyper-parameters are (0.1,0.4), (-0.1,0.3), (0.3,0.5), (-0.1,1). Here we have $K = 3$ subtypes, with cells in each subtype marked with a common color. **what are top and bottom rows?**

Supplementary Figure S7: Similar plots as Supplementary Figure S6, but for $K = 7$ subtypes

Supplementary Figure S8: Similar plots as Sumpplementary Figure S6, but for $K = 12$ subtypes

Supplementary Figure S9: $P(ED_g|X, y)$ given by scDDboost (horizontal) versus empirical Wasserstein distance (vertical). Genes associated with boxes from left to right having $P(ED_g|X, y)$ range from 0 - 0.2, 0.2 - 0.4, 0.4 - 0.6, 0.6 - 0.8, 0.8 - 1. For simulation cases with parameters in the format: number of clusters / shape / scale

Supplementary Figure S10: Roc curve of the 12 simulation settings, under each setting, TPR and FPR are averaged over ten replicates, generally `scDDboost` performs better than other methods

3.2. *Empirical Study.* In this section, we provide details of the empirical datasets and also demonstrate consistency to Wasserstein distance on one dataset FUCCI (Leng et al., 2015).

Data sets Details for the datasets used in the empirical studies with the estimated number of subtypes K are shown in Supplementary Table S1.

Data set	Conditions	Number of cells/condition	Organism	Ref	K
GSE94383	0 min unstim vs 75min stim	186,145	human	(Lane et al., 2017)	9
GSE48968-GPL13112	BMDC (2h LPS stimulation) vs 6h LPS	96,96	mouse	(Shalek et al., 2014)	4
GSE52529	T0 vs T72	69,74	human	(Trapnell et al., 2014)	7
GSE74596	NKT1 vs NTK2	46,68	mouse	(Engel et al., 2016)	7
EMTAB2805	G1 vs G2M	95,96	mouse	(Buettner et al., 2015)	6
GSE71585-GPL13112	Gad2tdTpositive vs Cux2tdTnegative	80,140	mouse	(Tasic et al., 2016)	4
GSE64016	G1 vs G2	91,76	human	(Leng et al., 2015)	6
GSE79102	patient1 vs patient2	51, 89	human	Kiselev et al. (2017)	4
GSE45719	16-cell stage blastomere vs mid blastocyst cell	50, 60	mouse	(Deng et al., 2014)	4
GSE63818	Primordial Germ Cells, develop- mental stage: 7 week gestation vs Somatic Cells, developmental stage: 7 week gestation	40,26	mouse	(Guo et al., 2015)	6
GSE75748	DEC vs EC	64, 64	human	(Chu et al., 2016)	5
GSE84465	neoplastic cells vs non-neoplastic cells	1000, 1000	human	(Darmanis et al., 2017)	9

SUPPLEMENTARY TABLE S1
Datasets used for empirical study

For the first 11 datasets in Supplementary Table S1 we use all the cells within that condition under same batch. The last one is the largest dataset we explored containing 3589 cells and comparing neoplastic cells (1091 cells) vs non-neoplastic cells (2498 cells). We randomly sampled 1000 cells from each condition, because it takes a lot of time for DESeq and scDD to compute when using all the samples and we conjecture that 1000 cells each condition would be enough to represent the heterogeneity. We run the comparison on those subsamples instead and found DESeq identified significantly smaller numbers of positives than other methods. It is intuitive that we are more likely to encounter subtle changes when we have large samples, and only considering mean shifts would have limited power.

We also observed consistent distributional change measurements by scDDboost and Wasserstein distance (Supplementary Figure S11).
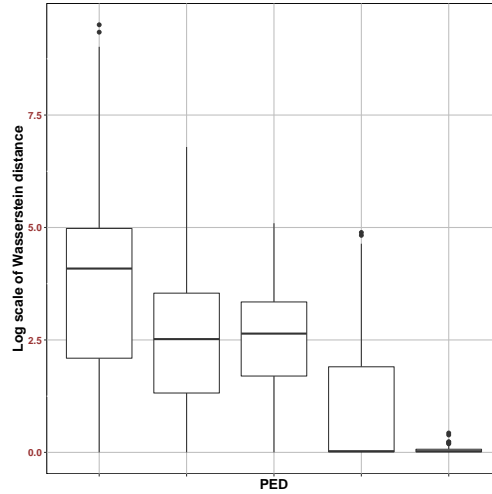
Supplementary Figure S11: $P(ED_g|X,y)$ given by scDDboost versus empirical Wasserstein distance. Genes associated with boxes from left to right having $P(ED_g|X,y)$ range from 0 - 0.2, 0.2 - 0.4, 0.4 - 0.6, 0.6 - 0.8, 0.8 - 1, data used: FUCCI

.

Datasets used for generating the Null cases are shown in Supplementary Table S2.

Data set	Conditions	Number of cells/condition	Organism
GSE63818null	7 week gestation	20,20	mouse
GSE75748null	DEC	32, 32	human
GSE94383null	T0	93, 93	human
GSE48968-GPL13112null	BMDC (2h LPS stimulation)	48,48	mouse
GSE74596null	NKT1	23,23	mouse
EMTAB2805null	G1	48,48	mouse
GSE71585-GPL13112null	Gad2tdTpositive	40,40	mouse
GSE64016null	G1	46,45	human
GSE79102null	patient1	26, 25	human

SUPPLEMENTARY TABLE S2

Datasets used for null cases, as cells are coming from same biological condition, there should not be any differential distributed genes, any positive call is false positive

3.3. *Bursting parameters.* Relevant material is reported in the main paper. This empty subsection is included to maintain labeling consistency.

3.4. *Time complexity.* Relevant material is reported in the main paper. This empty subsection is included to maintain labeling consistency.

3.5. *Diagnostics.*

3.5.1. *Negative binomial assumption.* We deploy a Pearson-type goodness-of-fit test (Yin and Ma (2013)) to check the adequacy of the negative binomial (NB) assumption in cell clusters from two data sets (EMTAB2805 and GSE45719). Supplementary Figure S12 presents the cumulative distribution of test p-values under each subtype, and indicates relatively little lack of fit. Among genes that demonstrate non-NB behavior, we find that most are handled the same way by scDDboost as by the standard comparison methods in terms of DD calls at 5% FDR. Supplementary Figures S13, and S14 display data from genes that show non-NB behavior and also are uniquely identified by scDDboost as being DD.

3.5.2. *Constant shape assumption: Likelihood ratio test.* As implemented, scDDboost treats the negative binomial mixture components as having constant shape within each gene. Here we investigate this assumption. Let σ^k be the shape parameter from subtype k We have null hypothesis
$$H_0 : \sigma^1 = \sigma^2 = \cdots = \sigma^K,$$
the test statistic is $2(l_1 - l_0)$, where l_1 is the log likelihood maximized over r and p given the data. l_0 is the log likelihood maximized under the H_0 constraint. We use simulation to verify the validity of the test. We simulate 500 random variables that are NB(3,0.5) distributed and another 500 random variables with distribution NB(3,0.7). Then test statistic and corresponding p value is recorded. We repeat the procedure for 100 times. Figure S15 shows that the p value is roughly uniform distributed

??? results in main??

3.5.3. *Clustering.* How sensitive are scDDboost results to the particular clustering methodology? To investigate, we applied the sc3 clustering method in place of the default in several numerical experiments. Following the original negative control experiment (main Figure 7), we applied scDDboost on each of five random splits of a number of data sets. In this case, we used five data sets: EMTAB2805, GSE64016, GSE93818, GSE74596, GSE71585. We observed zero positives by scDDboost at a 5% FDR call rate. We also checked scDDboost with sc3 in the simulation study (compare to Figures 4, 6, main). Here 5 replicate data sets were drawn in each setting. Supplementary Figure S16 shows that FDR is well controlled for the null genes.

4. Posterior consistency. In this section, we prove Theorem 4 and we discuss a case when condition (12) fails. The density of DDM is computed by product or ratio over several gamma functions. We use a crucial lemma which gives us an approximation to the gamma function, namely

Supplementary Figure S12: Cumulative distribution functions for subtype specific unadjusted p values of goodness of fit for NB distribution at two data sets(left is EMTAB2805, right is GSE45719), different colors are correspond to different subtypes

LEMMA 2. *For $x \geq 1$, $\frac{x^{x-c}}{e^{x-1}} \leq \Gamma(x) \leq \frac{x^{x-1/2}}{e^{x-1}}$, where $c = 0.577215...$ is the Euler-Mascheroni constant.*

PROOF OF LEMMA 2. By (Li and ping Chen, 2007), we have $\frac{x^{x-c}}{e^{x-1}} \leq \Gamma(x) \leq \frac{x^{x-1/2}}{e^{x-1}}$ for $x > 1$ and now we added the case when $x = 1, \Gamma(x) = 1$ so that both sides will include the equality case. $\square$

Supplementary Figure S13: Data set EMTAB2805, violin plot of the 57 genes having evidence against negative binomial distribution assumption and uniquely called positive under `scDDboost`

We have another lemma.

LEMMA 3. *If* $(\phi, \psi) \in A_{\pi_1} \cap A_{\pi_2}$, *follow the conditions in Theorem 1 then*

$$\frac{\omega_{\pi_1}^{post}}{\omega_{\pi_2}^{post}} \xrightarrow[n\to\infty]{a.s.} 0 \quad if \ N(\pi_1) < N(\pi_2)$$

PROOF OF LEMMA 3. Recall $\omega_{\pi}^{\text{post}} \propto p_{\pi}(t^1|t_{\pi}^1, y)\, p_{\pi}(t^2|t_{\pi}^2, y)\, p_{\pi}(t_{\pi}^1, t_{\pi}^2|y)\, \omega_{\pi}$ and RHS $= g(\pi, \alpha, \beta, n_1, n_2) f(\pi, t^1, t^2, \alpha, \beta)$ and $\frac{\omega_{\pi_1}^{\text{post}}}{\omega_{\pi_2}^{\text{post}}} = \frac{g(\pi_1, \alpha, \beta, n_1, n_2)}{g(\pi_2, \alpha, \beta, n_1, n_2)} \frac{f(\pi_1, t^1, t^2, \alpha, \beta)}{f(\pi_2, t^1, t^2, \alpha, \beta)}$ where

$$g(\pi, t^1, t^2, \alpha, \beta) = \left[\prod_{j=1}^{2}\prod_{b\in\pi}\frac{\Gamma(\Sigma_{k\in b}\alpha_k^j)}{\prod_{k\in b}\Gamma(\alpha_k^j)}\right]\frac{\Gamma(n_1+1)\Gamma(n_2+1)}{\prod_{b\in\pi}\Gamma(\beta_b)}\frac{\Gamma(\Sigma_{b\in\pi}\beta_b)}{\Gamma(n_1+n_2+\Sigma_{b\in\pi}\beta_b)}$$

$$f(\pi, t^1, t^2, \alpha, \beta) = \left[\prod_{j=1}^{2}\prod_{b\in\pi}\frac{1}{\prod_{k\in b}\Gamma(t_k^j+1)}\frac{\prod_{k\in b}\Gamma(\alpha_k^j+t_k^j)}{\Gamma(t_b^j+\Sigma_{k\in b}\alpha_k^j)}\right]\prod_{b\in\pi}\Gamma(\beta_b+t_b^1+t_b^2)$$

For notational simplicity, we use the abbreviation $g(\pi), f(\pi)$ to substitute

Supplementary Figure S14: Data set GSE45719, violin plot of the 13 genes having evidence against negative binomial distribution assumption and uniquely called positive under `scDDboost`

$g(\pi, \alpha, \beta, n_1, n_2), f(\pi, t^1, t^2, \alpha, \beta)$. We take log on $\frac{\omega_{\pi_1}^{post}}{\omega_{\pi_2}^{post}}$, denote it as LR. $LR = \log g(\pi_1) - \log g(\pi_2) + \log f(\pi_1) - \log f(\pi_2)$. Denote $C(\pi_1, \pi_2, \alpha, \beta) = \log g(\pi_1) - \log g(\pi_2)$, $C(\pi_1, \pi_2, \alpha, \beta)$ does not change with sample size n_1, n_2 and is a constant determined by partition π_1, π_2 and hyper parameters α, β. For further convenience of notation let $h(x) = \log \Gamma(x)$ and $\gamma_b^j = \Sigma_{k \in b} \alpha_k^j$. Denote $R(\pi_1, \pi_2, t^1, t^2, \alpha, \beta) = \log f(\pi_1) - \log f(\pi_2)$. And removing the common part of $f(\pi_1)$ and $f(\pi_2)$, we have

$$R(\pi_1, \pi_2, t^1, t^2, \alpha, \beta) = d(\pi_1, t^1, t^2, \alpha, \beta) - d(\pi_2, t^1, t^2, \alpha, \beta)$$

where

$$d(\pi, t^1, t^2, \alpha, \beta) = \sum_{b \in \pi} h(\beta_b + t_b^1 + t_b^2) - \sum_{j=1}^{2} \sum_{b \in \pi} h(t_b + \gamma_b^j)$$

Recall $\beta_b = \gamma_b^1 + \gamma_b^2$ and from Lemma 2, $(x - c)\log(x) - x + 1 \leq h(x) \leq (x - 1/2)\log(x) - x + 1$ we have

(5)

$$d(\pi, t^1, t^2, \alpha, \beta) \geq \sum_{b \in \pi}(\beta_b + t_b^1 + t_b^2 - c)\log(\beta_b + t_b^1 + t_b^2) - \sum_{j=1}^{2}\sum_{b \in \pi}(t_b^j + \gamma_b^j - 1/2)\log(t_b^j + \gamma_b^j) + N(\pi)$$

(6)

$$d(\pi, t^1, t^2, \alpha, \beta) \leq \sum_{b \in \pi}(\beta_b + t_b^1 + t_b^2 - 1/2)\log(\beta_b + t_b^1 + t_b^2) - \sum_{j=1}^{2}\sum_{b \in \pi}(t_b^j + \gamma_b^j - c)\log(t_b^j + \gamma_b^j) + N(\pi)$$

Supplementary Figure S15: cumulative distribution for p values of LRT

$$\text{RHS of (4)} = \Sigma_b \left[(t_b^1 + \gamma_b^1) \log(1 + \frac{t_b^2 + \gamma_b^2}{t_b^1 + \gamma_b^1}) + (t_b^2 + \gamma_b^2) \log(1 + \frac{t_b^1 + \gamma_b^1}{t_b^2 + \gamma_b^2}) \right.$$

$$\left. + (1 - c) \log(\beta_b + t_b^1 + t_b^2) - 1/2(\log(1 + \frac{t_b^2 + \gamma_b^2}{t_b^1 + \gamma_b^1}) + \log(1 + \frac{t_b^1 + \gamma_b^1}{t_b^2 + \gamma_b^2})) \right] + N(\pi)$$

By Taylor expansion at $x = 1$, $\log(x + 1) = \log(2) + 1/2(x - 1) - 1/8(x - 1)^2 + g(\xi)(x - 1)^3$, where $g(\xi)$ is the reminder term of form $\frac{1}{3(1+\xi)^3}$ for $0 < \xi < x$ For a fixed n_1, n_2, we have

$$\text{RHS of (4)} = (n_1 + n_2) \log(2) - \Sigma_{b \in \pi}(1/8(X_b^1 + X_b^2)$$
$$+ g(\xi_b)(Y_b^1 + Y_b^2)) + T(\pi) + N(\pi)$$

Supplementary Figure S16: FDR for simulation data sets, when using `scDDboost` with sc3 clustering

where $X_b^1 = \frac{(t_b^1 - t_b^2 + \gamma_b^1 - \gamma_b^2)^2}{t_b^1 + \gamma_b^1}$, $X_b^2 = \frac{(t_b^1 - t_b^2 + \gamma_b^1 - \gamma_b^2)^2}{t_b^2 + \gamma_b^2}$, $Y_b^1 = \frac{(t_b^1 - t_b^2 + \gamma_b^1 - \gamma_b^2)^3}{(t_b^1 + \gamma_b^1)^2}$, $Y_b^2 = \frac{(t_b^1 - t_b^2 + \gamma_b^1 - \gamma_b^2)^3}{(t_b^2 + \gamma_b^2)^2}$

and $T(\pi) = \Sigma_{b \in \pi} \left[(1-c) \log(\beta_b + t_b^1 + t_b^2) - 1/2(\log(1 + \frac{t_b^2 + \gamma_b^2}{t_b^1 + \gamma_b^1}) + \log(1 + \frac{t_b^1 + \gamma_b^1}{t_b^2 + \gamma_b^2})) \right]$

Similarly

$$\text{RHS of (5)} = (n_1 + n_2) \log(2) - \Sigma_{b \in \pi}(1/8(X_b^1 + X_b^2)$$
$$+ g(\xi_b)(Y_b^1 + Y_b^2)) + U(\pi) + N(\pi)$$

$$U(\pi) = \Sigma_{b \in \pi} \left[(2c - 1/2) \log(\beta_b + t_b^1 + t_b^2) - c(\log(1 + \frac{t_b^2 + \gamma_b^2}{t_b^1 + \gamma_b^1}) + \log(1 + \frac{t_b^1 + \gamma_b^1}{t_b^2 + \gamma_b^2})) \right]$$

Using above inequalities, we have

$$R(\pi_1, \pi_2, t^1, t^2, \alpha, \beta) \le U(\pi_1) - T(\pi_2) - 1/8(\Sigma_{b \in \pi_1}(X_b^1 + X_b^2) - \Sigma_{b \in \pi_2}(X_b^1 + X_b^2))$$
$$+ \Sigma_{b \in \pi_1} g(\xi_b)(Y_b^1 + Y_b^2) - \Sigma_{b \in \pi_2} g(\xi_b)(Y_b^1 + Y_b^2)$$

$Y_b^j = \frac{((t_b^1 - t_b^2 + \gamma_b^1 - \gamma_b^2)/\sqrt{n}))^3 / \sqrt{n}}{((t_b^j + \gamma_b^j)/n)^2}$, by LLN the denominator goes to a constant and by CLT in the numerator $(t_b^1 - t_b^2 + \gamma_b^1 - \gamma_b^2)/\sqrt{n} \to (t_b^1 - t_b^2)/\sqrt{n} \to \sqrt{n}[(t_b^1/n - \Phi_b) - (t_b^2/n - \Psi_b)]$, which converges to a normally distributed random variable when $\Phi_b = \Psi_b$. So Y_b^j is $o_p(1)$. Similarly, $X_b^j = \frac{((t_b^1 - t_b^2 + \gamma_b^1 - \gamma_b^2)/\sqrt{n})^2}{t_b^j + \gamma_b^j/n}$ is asymptotically gamma (χ-square) distributed. $g(\xi_b)$ has bounded variance, $U(\pi_1) - T(\pi_2) = -\log(n)$ if $N(\pi_2) < N(\pi_1)$ as $\log(\beta_b + t_b^1 + t_b^2) - \log(\beta_{b'} + t_{b'}^1 + t_{b'}^2) = \log(\frac{\beta_b + t_b^1 + t_b^2}{n}) - \log(\frac{\beta_{b'} + t_{b'}^1 + t_{b'}^2}{n}) \to O(1)$ *a.s.*, which completes the proof.

$\square$

PROOF OF THEOREM 4. Recall $\sum_{\pi \in \Pi} \omega_\pi^{\text{post}} = 1$ and $P(A_\pi | y, z) = \sum_{\tilde{\pi} \in \Pi} \omega_{\tilde{\pi}}^{\text{post}} 1[\tilde{\pi} \text{ refines } \pi]$. If $(\phi, \psi) \notin Q$, for all the A_π covers (ϕ, ψ) there is one finest π^* with the largest $N(\pi^*)$ and every other π that $(\phi, \psi) \in A_\pi$ is coarser than π^*. Theorem 4 now follows by Lemma 3.

$\square$

Under some choices of (ϕ, ψ), condition (12) could fail.

Supplementary Figure S17: Four subtypes of cells, simplexes of (ϕ, ψ) satisfying different constraints.

In Supplementary Figure S17, there are four subtypes, the rectangle with magenta boundary is a simplex $A_{\pi_1} = \{(\phi, \psi) : \phi_1 + \phi_2 = \psi_1 + \psi_2\}$, the rectangle with blue boundary is another simplex $A_{\pi_2} = \{(\phi, \psi) : \phi_1 + \phi_3 = \psi_1 + \psi_3\}$. The green line refers to $A_{\pi_3} = \{(\phi, \psi) : \phi_1 = \psi_1, \phi_2 = \psi_2\}$, the yellow line refers to $A_{\pi_4} = \{(\phi, \psi) : \phi_1 = \psi_1, \phi_3 = \psi_3\}$. the purple line refers to $O = \{(\phi, \psi) : \phi_1 + \phi_2 = \psi_1 + \psi_2, \phi_1 + \phi_3 = \psi_1 + \psi_3\}$, which is the intersection of A_{π_1} and A_{π_2}, and finally the black dot which is the intersection of those three lines refers to the simplex with finest partitions, $\phi_i = \psi_i, \forall i = 1, \cdots, 4$. When (ϕ, ψ) is from the purple line except the black dot, condition (12) would fail as there is not a finest π^* of $H(\phi, \psi)$. This may be of theoretical interest, but the practical implications of this finding are negligible as further computations have demonstrated.

References.

BUETTNER, F., NATARAJAN, K. N., CASALE, F. P., PROSERPIO, V., SCIALDONE, A., THEIS, F. J., TEICHMANN, S. A., MARIONI, J. C. and STEGLE, O. (2015). Computational analysis of cell-to-cell heterogeneity in single-cell RNA-sequencing data reveals hidden subpopulations of cells. *Nature Biotechnology* **33** 155 EP -.

CHU, L.-F., LENG, N., ZHANG, J., HOU, Z., MAMOTT, D., VEREIDE, D. T., CHOI, J., KENDZIORSKI, C., STEWART, R. and THOMSON, J. A. (2016). Single-cell RNA-seq reveals novel regulators of human embryonic stem cell differentiation to definitive endoderm. *Genome Biology* **17** 173. .

Dahl, D. B. (2009). Modal clustering in a class of product partition models. *Bayesian Anal.* **4** 243–264.

Darmanis, S., Sloan, S. A., Croote, D., Mignardi, M., Chernikova, S., Samghababi, P., Zhang, Y., Neff, N., Kowarsky, M., Caneda, C., Li, G., Chang, S. D., Connolly, I. D., Li, Y., Barres, B. A., Gephart, M. H. and Quake, S. R. (2017). Single-Cell RNA-Seq Analysis of Infiltrating Neoplastic Cells at the Migrating Front of Human Glioblastoma. *Cell reports* **21** 1399–1410.

Deng, Q., Ramsköld, D., Reinius, B. and Sandberg, R. (2014). Single-Cell RNA-Seq Reveals Dynamic, Random Monoallelic Gene Expression in Mammalian Cells. *Science* **343** 193–196.

Engel, I., Seumois, G., Chavez, L., Samaniego-Castruita, D., White, B., Chawla, A., Mock, D., Vijayanand, P. and Kronenberg, M. (2016). Innate-like functions of natural killer T cell subsets result from highly divergent gene programs. *Nature Immunology* **17** 728 EP -.

Guo, F., Yan, L., Guo, H., Li, L., Hu, B., Zhao, Y., Yong, J., Hu, Y., Wang, X., Wei, Y., Wang, W., Li, R., Yan, J., Zhi, X., Zhang, Y., Jin, H., Zhang, W., Hou, Y., Zhu, P., Li, J., Zhang, L., Liu, S., Ren, Y., Zhu, X., Wen, L., Gao, Y. Q., Tang, F. and Qiao, J. (2015). The Transcriptome and DNA Methylome Landscapes of Human Primordial Germ Cells. *Cell* **161** 1437–1452.

Jara, A., Hanson, T., Quintana, F., Müller, P. and Rosner, G. (2011). DPpackage: Bayesian Semi- and Nonparametric Modeling in R. *Journal of Statistical Software* **40** 1–30.

Kiselev, V. Y., Kirschner, K., Schaub, M. T., Andrews, T., Yiu, A., Chandra, T., Natarajan, K. N., Reik, W., Barahona, M., Green, A. R. and Hemberg, M. (2017). SC3: consensus clustering of single-cell RNA-seq data. *Nature Methods* **14** 483 EP -.

Lane, K., Van Valen, D., DeFelice, M. M., Macklin, D. N., Kudo, T., Jaimovich, A., Carr, A., Meyer, T., Pe'er, D., Boutet, S. C. and Covert, M. W. (2017). Measuring Signaling and RNA-Seq in the Same Cell Links Gene Expression to Dynamic Patterns of NF-B Activation. *Cell Systems* **4** 458–469.e5.

Leng, N., Dawson, J. A., Thomson, J. A., Ruotti, V., Rissman, A. I., Smits, B. M. G., Haag, J. D., Gould, M. N., Stewart, R. M. and Kendziorski, C. (2013). EBSeq: an empirical Bayes hierarchical model for inference in RNA-seq experiments. *Bioinformatics* **29** 1035-1043.

Leng, N., Chu, L.-F., Barry, C., Li, Y., Choi, J., Li, X., Jiang, P., Stewart, R. M., Thomson, J. A. and Kendziorski, C. (2015). Oscope identifies oscillatory genes in unsynchronized single-cell RNA-seq experiments. *Nature Methods* **12** 947 EP -.

Li, X. and ping Chen, C. (2007). Inequalities for the gamma function. In *2007), Art. 28. [ONLINE: http://jipam.vu.edu.au/article.php?sid=842.*

Ray, S. and Turi, R. H. (2000). Determination of Number of Clusters in K-Means Clustering and Application in Colour Image Segmentation.

Shalek, A. K., Satija, R., Shuga, J., Trombetta, J. J., Gennert, D., Lu, D., Chen, P., Gertner, R. S., Gaublomme, J. T., Yosef, N., Schwartz, S., Fowler, B., Weaver, S., Wang, J., Wang, X., Ding, R., Raychowdhury, R., Friedman, N., Hacohen, N., Park, H., May, A. P. and Regev, A. (2014). Single-cell RNA-seq reveals dynamic paracrine control of cellular variation. *Nature* **510** 363 EP -.

Tasic, B., Menon, V., Nguyen, T. N., Kim, T. K., Jarsky, T., Yao, Z., Levi, B., Gray, L. T., Sorensen, S. A., Dolbeare, T., Bertagnolli, D., Goldy, J., Shapovalova, N., Parry, S., Lee, C., Smith, K., Bernard, A., Madisen, L., Sunkin, S. M., Hawrylycz, M., Koch, C. and Zeng, H. (2016). Adult mouse cortical cell taxonomy revealed by single cell transcriptomics. *Nature Neuroscience* **19** 335 EP -.

Trapnell, C., Cacchiarelli, D., Grimsby, J., Pokharel, P., Li, S., Morse, M., Lennon, N. J., Livak, K. J., Mikkelsen, T. S. and Rinn, J. L. (2014). The dynamics and regulators of cell fate decisions are revealed by pseudotemporal ordering of single cells. *Nature biotechnology* **32** 381–386.

Yin, G. and Ma, Y. (2013). Pearson-type goodness-of-fit test with bootstrap maximum likelihood estimation. *Electronic journal of statistics* **7** 412–427.